In-situ nanofabrication of hybrid PEG-dendritic – inorganic nanoparticles and preliminary evaluation of their biocompatibility

Ana Sousa-Herves,[a] Christian Sánchez Espinel,[b] Amir Fahmi,*[c] África González-Fernández*[d] and Eduardo Fernandez-Megia*[a]

Received (in XXX, XXX) Xth XXXXXXXXX 20XX, Accepted Xth XXXXXXXXX 20XX
DOI: 10.1039/b000000x

An *in-situ* template fabrication of inorganic nanoparticles using carboxylated PEG-dendritic block copolymers of the GATG family is described as a function of the dendritic generation, the metal (Au, CdSe) and metal molar ratio. The biocompatibility of the generated nanoparticles analysed in terms of their aggregation in physiological media, cytotoxicity and uptake by macrophages relates to the PEG density of the surface of the hybrids.

Introduction

Hybrid organic-inorganic nanoparticles (NPs) are innovative nanomaterials that attract great attention due to their unique properties in scientific research and industry. By combining the functionality of inorganic particles and the flexibility of organic templates, hybrid materials are obtained with distinct physicochemical properties for applications in biotechnology,[1] memory devices,[2] and sensors.[3,4] Linear block copolymers are convenient organic matrices to template a variety of inorganic NPs with good control over size and particle size distribution.[5, 6] When appropriately designed, block copolymers result in phase-separated nanodomains with different morphologies that can direct the assembly of metallic NPs into well-defined architectures with unique mechanical, optical, magnetic and electronic properties.[7] Dendrimers have also received much attention as macromolecular hosts to template inorganic NPs by exploiting their characteristic highly functional surface and globular architecture in the nanometer scale.[8-12] We envisaged that appropriately functionalized linear-dendritic copolymers[13] could bring together the favourable properties of dendrimers and block copolymers to template the fabrication of inorganic NPs and improve their colloidal stability and biocompatibility in physiological media. It has been reported that organosoluble linear-dendritic copolymers prepared by RAFT can disperse previously formed metallic NPs (TiO_2, Au, CdSe) in organic solvents and a polymeric matrix.[14] We hypothesised that the incorporation of the hydrophilic, FDA-approved poly(ethylene glycol) (PEG) as linear block could not only assist the template *in-situ* fabrication of NPs, but also enhance their aqueous solubility and stealth properties for biomedical applications.

Thus, it is well known that the incorporation of PEG at the focal point of dendrimers results in customizable platforms where the careful selection of the PEG length, the nature of the peripheral groups, and the structure and generation of the dendritic block entail materials for specific applications in the biomedical field.[15] Indeed, polymeric micelles,[16,17] hydrogels,[18,19] and polymer–drug conjugates[20,21] have been described from PEG-dendritic block copolymers for drug delivery, diagnosis, and tissue engineering.

Herein we describe a straightforward *in-situ* route to generate biocompatible inorganic NPs templated by three generations (G1, G2, G3) of PEG-dendritic block copolymers of the GATG (gallic acid-triethylene glycol) family[22] functionalized with peripheral carboxylate groups (Scheme 1). GATG dendrimers have recently emerged as a modular and versatile platform in the biomedical field with applications[23,24,25] in drug and gene delivery,[26,27,28,29] diagnosis,[30] antiviral agents,[31] or for the treatment of neurodegenerative diseases.[32] The presence of terminal azides on GATG facilitates their efficient decoration with a variety of ligands by means of the Cu(I)-catalyzed azide–alkyne cycloaddition (CuAAC).[33,34,35, 36] The selection of carboxylates for the present purpose is based on their ability to complex metal ions and so direct the formation of hybrid dendritic materials. Two types of NPs have been prepared, namely noble metal Au and semiconductor CdSe. The potential of these NPs for biomedical applications has been preliminary assessed by studying their stability in serum, cytotoxicity, and phagocytosis as a function of G, the metal, and the carboxylate:metal molar ratio.

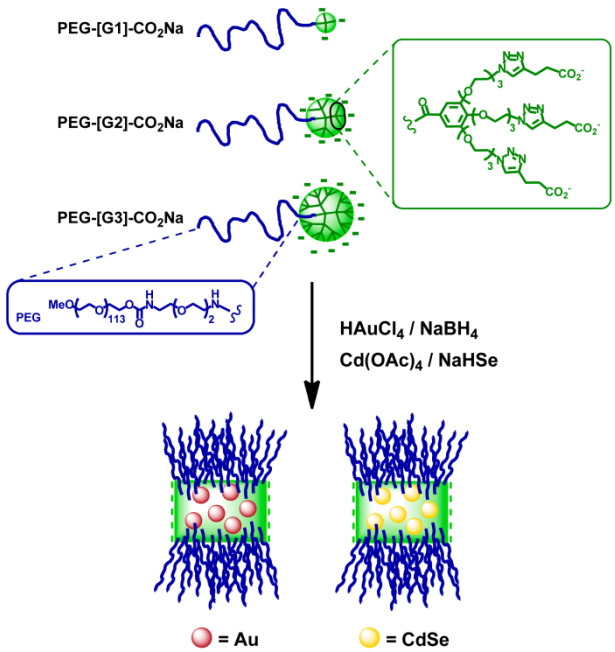

Scheme 1. Schematic representation of the preparation of metallic NPs templated by carboxylated PEG-GATG block copolymers.

Experimental

Materials and Methods. $CuSO_4 \cdot 5H_2O$ and sodium bicarbonate were obtained from Prolabo. Sodium ascorbate was purchased from Acros Organics. 4-pentynoic acid and *t*-BuOH were obtained from Sigma-Aldrich. MeO-PEG_{5000}-OH (M_n 5055.5, M_w 5087.8 by MALDI-TOF) was purchased from Fluka. H_2O was of Milli-Q grade. All other reagents were of analytical grade. Ultrafiltration was performed on stirred cells with Amicon® YM3 membranes. NMR spectra were recorded on a Bruker DRX 500 MHz. Chemical shifts are reported in ppm (δ units) downfield from internal HOD signal (D_2O). FT-IR (KBr) spectra were recorded on a Bruker IFS-66v. Gel permeation chromatography (GPC) experiments were performed using a PSS Suprema Lux precolumn (10 µm, 8 x 50 mm) and a PSS Suprema Lux column (10 µm, 100 Å, 8 × 300 mm) with a UV detector (254 nm). A 10 mM phosphate buffer pH 8.2 solution supplemented with 150 mM LiCl was used as eluent at 1.0 mL/min. Solutions at 0.5-1.0 mg/mL were filtered through 0.45 µm before injection. Dynamic light scattering (DLS) measurements were performed on a Malvern Nano ZS (Malvern Instruments) operating at 633 nm with a 173º scattering angle. Solutions at 1.0 mg/mL in 10 mM phosphate buffer pH 8.2 supplemented with 150 mM LiCl were filtered through 0.45 µm before analysis. UV-Vis spectra were recorded on a Varian Cary 50 and Varian Eclipse photospectrometer; the monochromator slit width was 5 nm. For TEM measurements, thin films of the solutions (0.3 mM) were spin-coated on carbon coated copper grids (400 mesh / AGAR Scientific) using a solid substrate support. The copper grid was then peeled of the substrate and analysed in a TECNAI BioTWIN (FEI Ltd.) transmission electron microscope at 100kV. The instrument was operated at low beam intensities to prevent electron damage of the polymer samples. HR-TEM measurements were performed using a JEOL JEM-2110F operated at 200kV; the instrument was equipped with an Orius SC1000 digital camera. The content of Au on macrophages was analysed by inductively coupled plasma mass spectrometry (ICP-MS) on a Neptune MC-ICP-MS (Thermo Scientific).

Synthesis of carboxylated PEG-dendritic block copolymers. PEG_{5000}-[Gn]-N_3 was dissolved in *t*-BuOH-H_2O (1:1) at a final 0.1 M concentration of terminal azides. Then, 4-pentynoic acid (200 mol% per N_3), $NaHCO_3$ (220 mol% per N_3) and freshly prepared aqueous solutions of $CuSO_4$ (5 mol% per N_3) and sodium ascorbate (25 mol% per N_3) were added. After 48 h of stirring at rt protected from light, reaction mixtures were purified by ultrafiltration (Amicon® YM3) washing with pH 2 aq HCl (2 x 30 mL), sat $NaHCO_3$ (2 x 30 mL), and H_2O (4 x 30 mL) to afford PEG-[Gn]-CO_2Na as white foams after freeze-drying.

PEG-[G1]-CO_2Na: PEG-[G1]-N_3 (115 mg, 19.7 µmol), 4-pentynoic acid (11.6 mg, 118 µmol), $NaHCO_3$ (10.9 mg, 130 µmol), sodium ascorbate (2.91 mg, 14.7 µmol), and $CuSO_4$ (0.73 mg, 2.95 µmol) were dissolved in *t*-BuOH (0.33 mL)-H_2O (0.33 mL), and following the general procedure described above, PEG-[G1]-CO_2Na (121 mg) was obtained in 99% yield. IR (KBr, cm^{-1}) 3426, 2887, 1666, 1581, 1115. ^1H NMR (500 MHz, D_2O) δ: 7.79 (s, 1H), 7.78 (s, 2H), 7.18 (s, 2H), 4.59-4.49 (m, 6H), 4.30-4.12 (m, 8H), 3.97-3.52 (m, 542 H), 3.41 (s, 3H), 3.28 (t, J = 4.89 Hz, 2H), 2.94-2.84 (m, 6H), 2.54-2.44 (m, 6H). ^{13}C NMR (75 MHz, D_2O) δ: 181.9, 170.1, 162.3, 158.9, 152.5, 148.2, 140.3, 129.7, 123.8, 106.9, 72.7, 71.6, 71.2, 70.7, 70.3, 70.1, 70.0, 69.9, 69.7, 69.5, 69.4, 69.1, 69.0, 58.6, 50.4, 40.6, 40.0, 37.4, 22.3.

PEG-[G2]-CO_2Na: PEG-[G2]-N_3 (111 mg, 14.5 µmol), 4-pentynoic acid (25.7 mg, 263 µmol), $NaHCO_3$ (24.1 mg, 280 µmol), sodium ascorbate (6.45 mg, 32.6 µmol), and $CuSO_4$ (1.63 mg, 6.50 µmol) were dissolved in *t*-BuOH (0.66 mL)-H_2O (0.66 mL), and following the general procedure described above, PEG-[G2]-CO_2Na (113 mg) was obtained in 90% yield. IR (KBr, cm^{-1}) 3408, 2887, 1650, 1581, 1114. ^1H NMR (500 MHz, D_2O) δ: 7.78 (s, 3H), 7.76 (s, 6H), 7.15-7.03 (m, 8H), 4.52 (br s, 18H), 4.20-4.02 (m, 20H), 3.99-3.51 (m, 693 H), 3.41 (s, 3H), 3.20 (br s, 2H), 2.94-2.83 (m, 18H), 2.54-2.44 (m, 18H). ^{13}C NMR (75 MHz, D_2O) δ: 181.5, 168.8, 151.9, 147.7, 139.8, 129.8, 123.5, 106.2, 72.0, 70.9, 70.6, 69.4, 69.0, 68.7, 68.4, 68.2, 58.1, 49.7, 39.5, 36.7, 21.7.

PEG-[G3]-CO_2Na: PEG-[G3]-N_3 (78 mg, 6.0 µmol), 4-pentynoic acid (32.0 mg, 326 µmol), $NaHCO_3$ (30.2 mg, 359 µmol), sodium ascorbate (8.08 mg, 40.8 µmol), and $CuSO_4$ (2.00 mg, 8.20 µmol) were dissolved in *t*-BuOH (0.82 mL)-H_2O (0.82 mL), and following the general procedure described above, PEG-[G3]-CO_2Na (98 mg) was obtained in 99% yield. IR (KBr, cm^{-1}) 3400, 2876, 1646, 1581, 1114. ^1H NMR (500 MHz, D_2O) δ: 7.87-7.65 (m, 27H), 7.09 (s, 26H), 4.62-4.40 (m, 54H), 4.32-3.99 (m, 80H), 3.97-3.46 (m, ~966H), 3.41 (m, 5H), 2.97-2.77 (m, 54H), 2.59-2.35 (m, 54H).

Nanoparticle Preparation. Carboxylated PEG-[Gn]-CO_2Na copolymers were used to prepare metallic Au and semiconductor CdSe NPs. Firstly, PEG-[Gn]-CO_2Na of G1, G2, and G3 were dissolved in aqueous media at a concentration of 0.3 mM.

For the preparation of Au NPs, an Au precursor ($HAuCl_4$) was added to the polymer solutions at molar ratios 1:1 and 3:1 with respect to the number of carboxylate end-groups. $HAuCl_4$ was then reduced to metallic Au^0 using a three-fold molar excess of aqueous 0.1 M $NaBH_4$. Upon addition of the reducing agent, the solutions turned ruby red indicating the formation of Au NPs.

For the preparation of CdSe NPs, firstly, $Cd(OAc)_2$ was added to the copolymer solutions in molar ratios 1:1 and 3:1 with respect to the number of carboxylate end-groups. Then, a fresh solution of 5 mM NaHSe in anhydrous EtOH was prepared by reaction of Se powder with $NaBH_4$ under inert atmosphere. CdSe NPs were formed upon injecting the NaHSe solution into the aqueous solution containing Cd(II) under inert atmosphere and vigorous stirring. The solutions turned brightly yellow-orange indicating the formation of semiconductor CdSe nanoclusters.

Aggregation studies. 50 µg/mL of NPs in RPMI with 10% fetal calf serum (FCS) were incubated overnight at 37 ºC and the formation of aggregates was evaluated in an optical inverted microscope (model IX50 Olympus Optical Co, GMBH, Germany). Amplification: 40x objective.

Cellullar experiments. For toxicology analysis, the human tumour cell lines Hmy2 and U937 were used, which correspond to lymphoblastoid B and myeloid-monocytic lymphoma (myeloid origin) cell lines, respectively. All cells were maintained in RPMI (Gibco, Life Technologies, Grand Island) supplemented with 10 wt. % heat inactivated FCS (PAA, Linz, Austria), penicillin (100 U/mL), streptomycin (100 µg/mL) and glutamine (2 mM) (Gibco) at 37 ºC in a humidified atmosphere containing 5 vol % CO_2. Mouse peritoneal macrophages were collected by flushing with

PBS the peritoneal cavity of C57BL6 mice. Recovered cells were centrifuged for 5 min at 231 g and resuspended in RPMI containing 10% heat inactivated FCS.

Cellular proliferation colorimetric assay. Previous to perform the viability assays, the optimal cell number per well (from 5.000 up to 35.000 cells) was determined at 24 and 48 h. The number of cells in which the absorbance reached an exponential growing of cells, was considered optimal. Cells were treated with the Quick Cell proliferation testing solution (GenScript Corporation, Piscataway, NJ, USA), following manufacturer instructions. Briefly, after incubation, plates were centrifuged at 1000 g for 1 min, 100 µL of the supernatant were discarded and 50 µL of Quick Cell reagent added. Then, plates were incubated for 3 h at 37 ºC, centrifuged again and supernatants were transferred to clean plates. All assays were performed twice for each cell line, at 24 and 48 h, and in triplicate for each NPs concentration. The absorbance was measured at 450 nm in a microplate reader (MULTISKAN EX. BioAnalysisLabsystems). For viability assays, cells were incubated in the presence of 0.5 µg/mL or 50 µg/mL of NPs for 24 and 48h, and the viability was analyzed following the equation:

$$\%\text{viability} = \frac{\text{Sample absorbance (cells+NPs)} - \text{NPs absorbance}}{\text{Cells absorbance} - \text{RPMI absorbance}} \times 100$$

Phagocytosis studies using mouse macrophages. The protocol was adapted to the guidelines of the Spanish regulations (Royal Decree 53/2013) regarding the use of animals in scientific research and under the approval of the ethical committee of the University of Vigo (Spain) (number 03/11). Peritoneal macrophages were plated in 24-well plates (Becton Dickinson, Franklin Lakes, USA). After 1 h of incubation at 37 ºC in a humidified atmosphere, hybrid NPs were added to the cells and incubated overnight at 37 ºC with 5 vol % CO_2. Macrophages were washed several times with PBS and then 100 µL of H_2O were added to kill the cells. Cell lysates in H_2O were collected for ICP-MS assay and the concentration of phagocyted Au (per 100 µg/mL of hybrids) was measured.

Results and discussion

Three generations of PEG-GATG copolymers carrying 3, 9, and 27 carboxylate groups (PEG-[Gn]-CO_2Na, n=1,2,3) where readily prepared by CuAAC from the corresponding PEG-[Gn]-N_3 (90-99% yield, PEG_{5000}, Figure S1 in the ESI).[29,37] Complete functionalization of the copolymers was demonstrated by IR (disappearance of the intense characteristic azide signal at 2107 cm^{-1}) and ^1H NMR (D_2O, appearance of two singlets at *ca.* 7.8 ppm in a ratio 1:2 corresponding to the triazol protons and a multiplet around 4.5 ppm characteristic of the methylene protons adjacent to the triazol ring). Gel permeation chromatography (GPC) confirmed the integrity and purity of the products, in addition to the expected increase in size with generation (Figure 1). These materials showed complete aqueous solubility. As seen in Figures 1 and S2, no sign of aggregation was observed by dynamic light scattering (DLS) which in agreement with GPC revealed an increase in mean hydrodynamic diameter on going from G1 (4.6 nm) to G2 (5.4 nm) and G3 (6.8 nm). Because of their high solubility and the absence of aggregation, PEG-[Gn]-CO_2Na were readily used for the preparation of NPs, namely Au and CdSe. These NPs have recently attracted much attention in the biomedical field due to their optical and luminescence properties with interesting applications in drug and gene delivery, hyperthermia treatment and tumour ablation in cancer therapy.[38]

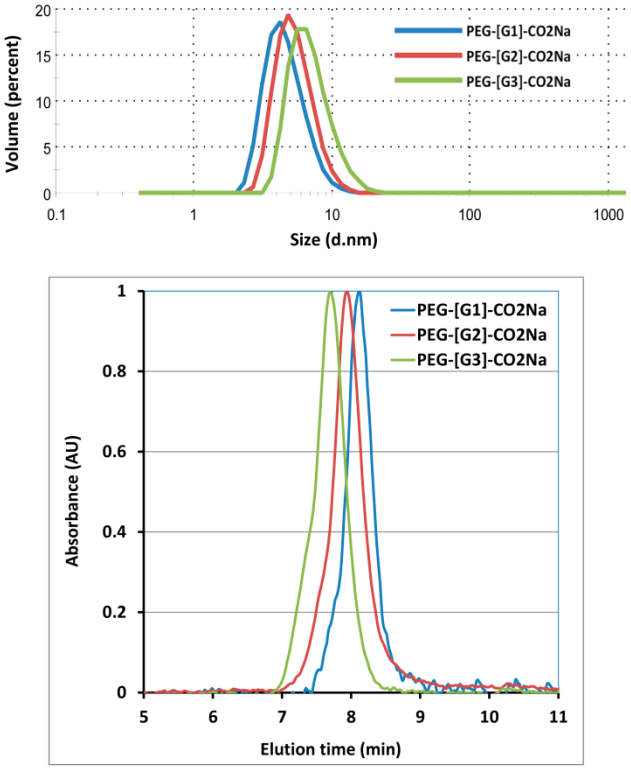

Figure 1. DLS size distribution and normalized GPC elugrams of PEG-[Gn]-CO_2Na (10 mM phosphate buffer pH 8.2, 150 mM LiCl).

Templated preparation of hybrid PEG-GATG – Au NPs. Au NPs were synthesized in a two-step process comprising extraction of aqueous $AuCl_4^-$ into the carboxylated GATG block, followed by reduction with $NaBH_4$. The efficiency of PEG-GATG to template NPs by this *in-situ* approach was evaluated by UV–vis and transmission electron microscopy (TEM). Both measurements were conducted for G1-G3 using molar ratios 1:1 and 1:3 between the carboxylate groups on the dendritic block and the inorganic $HAuCl_4$ precursor. Figure 2 shows typical UV–vis spectra of Au NPs (50 µg/mL) prepared within the PEG-GATG matrix. The plasmon peak at around 525 nm observed for all samples is attributed to collective oscillation of free electrons in Au NPs.[39] The gradual increase of absorption below 400 nm is due to the inter-band transition of Au. The absorbance peak at 285 nm for all NPs is assigned to the characteristic ion-pair formation between $AuCl_4^-$ and the PEG-dendritic copolymers after adding the Au-precursor.[9, 40]

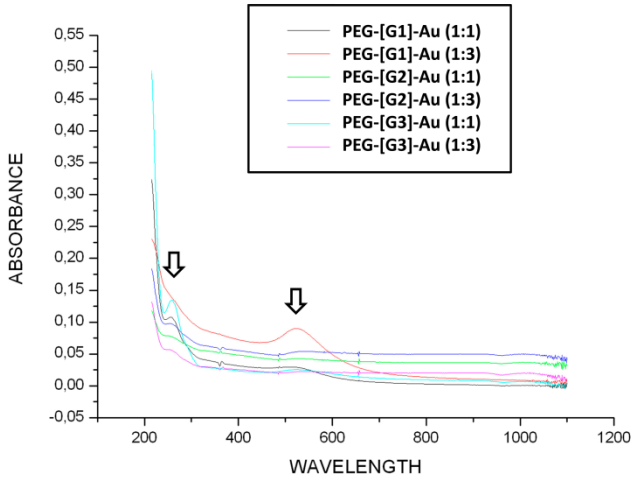

Figure 2. UV-vis spectra of PEG-GATG – Au NPs showing a plasmon band at 525 nm and a shoulder at 285 nm.

TEM micrographs in Figure 3 show Au NPs (ratio 1:1) with average size in the range 4-10 nm. NPs templated within G1 reveal irregular shape and average size 8±1.5 nm. On increasing the dendrimer generation, the templating effect of the dendritic block becomes dominant, resulting in average sizes 6±1.2 and 4±1 nm for G2 and G3, respectively. It is proposed that the larger G1 NPs are produced by overlapping of two or more smaller particles that in the two-dimensional HRTEM projection appear as a single one (Figure S3). It seems that in G1, the generated Au NPs are partially coated with dendritic wedges which lead to a high surface energy and aggregation to form larger particles. The use of the G2 and G3 copolymers results in an enhanced control over the particle growth and smaller NPs. This is attributed to a more effective passivation of the generated NPs within the dendritic matrices, a mechanism contributing to avoid flocculation probably *via* steric stabilisation.[41]

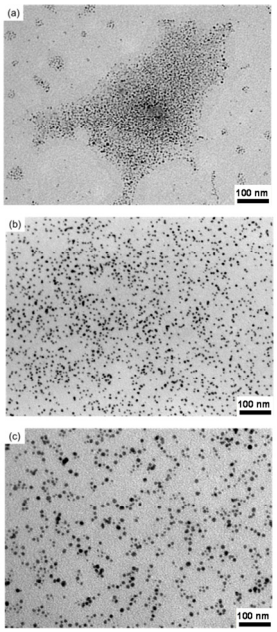

Figure 3. TEM of Au NPs templated by carboxylated PEG-GATG. (a) PEG-[G1]-Au (1:1), (b) PEG-[G2]-Au (1:1), (c) PEG-[G3]-Au (1:1).

PEG-GATG templates CdSe NPs. CdSe NPs were prepared by injection of NaHSe to carboxylated PEG-GATG previously complexed with $Cd(OAc)_2$ in aqueous solution. $Cd(OAc)_2$ was added to G1-G3 copolymers in molar ratios carboxylate to Cd, 1.1 and 1:3. Figure 4 displays photoluminescence emission spectra of CdSe NPs (excitation at 360 and 380 nm) showing emissions with maxima at 480 and 510 nm, respectively, which correspond to electron-hole radiative recombination from trap states. The peak of NPs templated within G3 at 480 nm is narrow and of high intensity, reflecting CdSe NPs with low polydispersity. The peaks around 510 nm for G1 and G2 are wider than G3, refereeing to larger NPs and higher dispersity.[12, 42, 43] These results point again to a generation dependent stabilisation mechanism of NPs in the template process also confirmed by TEM.

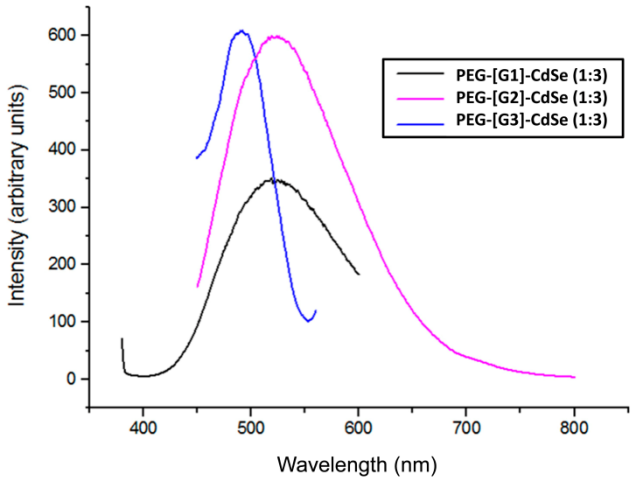

Figure 4. Photoluminescence spectra of CdSe NPs templated within carboxylated PEG-GATG copolymers.

TEM micrographs of the NPs are shown in Figure 5. Particles stabilised within G1 possess not uniform morphologies with average size 8±1.5 nm. As previously observed for Au, CdSe NPs stabilised by G2 and G3 markedly revealed smaller in size (5±0.1nm), consistent again with the existence of a generation dependent mechanisms to template the NPs. In the case of the smaller particles, PEG-GATG acts as a nanoreactor controlling the growth of the CdSe NPs within defined dendritic cavities. On the contrary, the alignment of the smaller G1 wedges on the NP surface results in a lower control over size.[44]

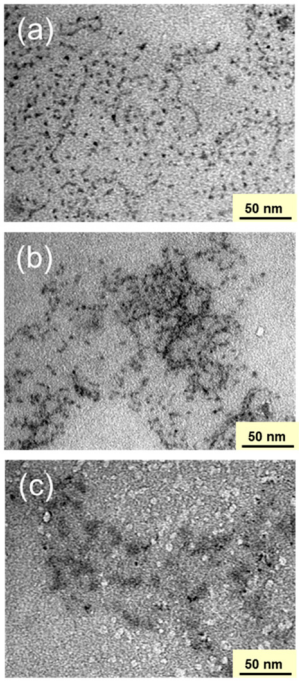

Figure 5. TEM of (a) PEG-[G1]-CdSe (1:3), (b) PEG-[G2]-CdSe (1:3), (c) PEG-[G3]-CdSe (1:3).

Aggregation in physiological media depends on the dendritic block generation. Since nanostructures for *in vivo* applications should be biocompatible and not aggregate in the presence of serum proteins, we decided to analyse the behaviour of the NPs in physiological media. Accordingly, all NPs were incubated in the presence of media supplemented with fetal calf serum (FCS) at 37 ºC with 5% of CO_2. As seen in Table 1 and Figures 6 and S4, optical microscopy showed the presence of aggregates at higher dendrimer G and on increasing the carboxylate:metal molar ratio from 1:1 to 1:3. The increased aggregation observed at higher G can be explained by the lower PEG density on the surface of these hybrids. Indeed, the architecture of dendronized Au and CdSe NPs has been claimed as controlled by a sterically induced stoichiometry,[45] where the relative size between the metal core and the dendrimers on the shell determines the core-shell stoichiometry by steric reasons.[46,47] In this scenario, an increased number of PEG-dendritic copolymers of lower G is expected to accommodate around the metal core, resulting in a higher PEG density and enhanced stability towards aggregation with serum proteins. This situation is similar to that seen in PEG-GATG–based dendriplexes previously described by our group (a pDNA core surrounded by a shell of dendrimers) where the lower G copolymers afford a more effective shielding of the surface charge because of a denser PEG palisade.[27, 28] The lower PEG content also explains the larger aggregation seen on increasing the carboxylate:metal molar ratio.

Table 1: Aggregation of metal NPs in the presence of serum analyzed by optical microscopy (50 μg/mL of NPs in RPMI supplemented with 10% FCS)

METAL	NPS	Aggregation (*in vitro*)
Au	PEG-[G1]-Au (1:1)	−
	PEG-[G1]-Au (1:3)	±
	PEG-[G2]-Au (1:1)	+
	PEG-[G2]-Au (1:3)	++
	PEG-[G3]-Au (1:1)	+
	PEG-[G3]-Au (1:3)	++
CdSe	PEG-[G1]-CdSe (1:1)	+
	PEG-[G1]-CdSe (1:3)	++
	PEG-[G2]-CdSe (1:1)	+
	PEG-[G2]-CdSe (1:3)	++
	PEG-[G3]-CdSe (1:1)	+
	PEG-[G3]-CdSe (1:3)	++

++, +, ±, − refer to high, medium, low, and no aggregation.

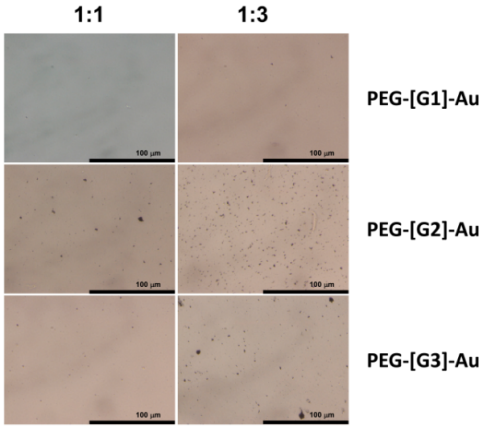

Figure 6. Aggregation of Au NPs in the presence of serum by optical microscopy (40x objective).

NPs display low toxicity. The biocompatibility of the less aggregating NPs was further assessed in cell toxicity experiments at 24 and 48 h with no statistical differences between them. Thus, PEG-[G1,2,3]-Au (1:1), PEG-[G1]-Au (1:3) and PEG-[G1,2,3]-CdSe (1:1) hybrids were tested in Hmy2 (Figure 7) and U937 (not shown) cell lines. The toxicity of the three generation block copolymers was also studied, revealing non-toxicity after 48 h of incubation with the cells (Figure S5). Following the Nanotechnology Characterization Laboratory criteria regarding toxicity[48] (cell viability higher than 75% at 48 h), it can be concluded that the tested Au NPs showed null or very low cytotoxicity on human cells (Figure 7). This result is in agreement with previous reports from several groups,[49] including ours,[50] on the relative lack of toxicity of conventional Au NPs. It was also interesting to see the good viability results obtained with PEG-[G1]-CdSe (1:1) considering the high toxicity traditionally associated to CdSe systems.[51, 52] On increasing G, however, toxicity was induced in CdSe NPs at the highest concentration tested (50 μg/mL), a result confirming again the higher biocompatibility of the lower G hybrids as a result of their increased PEG content.

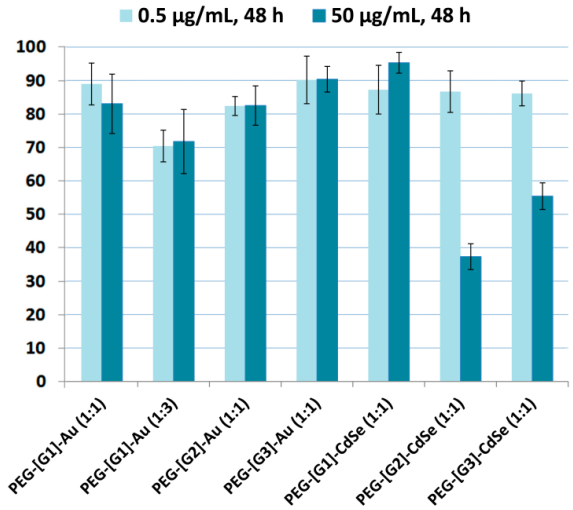

Figure 7. Cell viability of the Hmy2 cell line at 48 h in the presence of several NPs.

Phagocytosis. Innate immune cells such as macrophages are very active cells in the uptake and quick removal of nanostructures from circulation.[53, 54] For instance, in the case of Au, it is known that the scavenger receptor A mediates the uptake of Au colloids by macrophages.[55] PEGylation has been proposed as an effective way to grant nanostructures with stealth properties and hence, prolong their circulation times.[56, 57] In order to further asses the behaviour of the sterically stabilized hybrids herein reported in the presence of phagocytic cells, we have studied the uptake of the PEG-[G1,2,3]-Au (1:1) structures in normal peritoneal mouse macrophages. Thus, the hybrids were added on top of cells, and after incubation and several washes, the amount of Au was analysed by ICP-MS in the cell lysates. The results show in all cases very low concentration of Au inside the cells, in agreement with the hybrids being not highly internalized (Figure 8). Relatively higher capture efficiency was however observed for PEG-[G2]-Au and PEG-[G3]-Au. Although it is not possible to exclude this higher uptake as related to properties like the size or aggregation of these hybrids in physiological media, it cannot be ignored its close correlation with their lower density of PEG compared to G1, a result that stresses again the reduction of cell uptake and potential toxic effects imparted by PEG to nanomaterials.[58, 59]

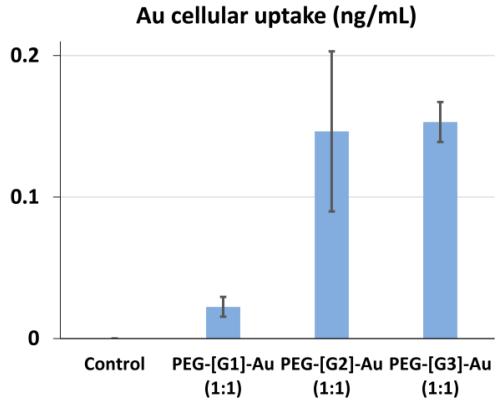

Figure 8. Phagocytosis of Au NPs by macrophages determined by ICP-MS in cell lysates.

Conclusions

Three generations of PEG-dendritic block copolymers of the GATG family functionalized with peripheral carboxylates have been used to template different types of inorganic (Au and CdSe) NPs by an *in-situ* reduction approach. A generation dependent template mechanism was confirmed that results in an enhanced control over the particle growth and smaller sizes on increasing the dendritic generation (G). On the other hand, the higher biocompatibility of the lower G hybrids is interpreted as a result of the characteristic architecture of these metallic NPs controlled by a sterically induced stoichiometry. The presence of a single PEG chain in the block copolymers (irrespective of G) ensues a denser PEG palisade around the metal core for the lower G hybrids, that finally leads to a reduced aggregation in physiological media, cytotoxicity and uptake by macrophages. Based on these results, the incorporation of higher molecular weight PEG chains is envisioned as a prospective way to grant these hybrids with enhanced steric stabilization.

Acknwoledgments

C.S.E. and A.G.-F. thank to the European Commission BIOCAPS (316265, FP7/REGPOT-2012-2013.1) and Xunta de Galicia (Agrupamento INBIOMED and Grupo con potencial crecimiento). A.S.-H. and E.F.-M. thank the Spanish Government (CTQ2012-34790) and the Xunta de Galicia (CN2011/037).

Notes and references

[a] *Department of Organic Chemistry and Center for Research in Biological Chemistry and Molecular Materials (CIQUS), University of Santiago de Compostela, Jenaro de la Fuente s/n, 15782, Santiago de Compostela, Spain. Tel: +34 8818 15727; E-mail: ef.megia@usc.es*

[b] *NanoImmunoTech (NIT) Edificio CITEXVI, Fonte das Abelleiras 36310, Vigo, Spain.*

[c] *Faculty of Technology and Bionics, Rhein-Waal University of Applied Sciences, Marie-Curie-Straße 1, D-47533 Kleve, Germany. E-mail: Amir.Fahmi@hochschule-rhein-waal.de*

[d] *Immunology, Institute of Biomedical Research (IBI), Biomedical Research Center (CINBIO), University of Vigo, Campus Lagoas Marcosende, 36310, Vigo, Spain. Tel: +34 986 812625; E-mail: africa@uvigo.es*

† Electronic Supplementary Information (ESI) available: Structure of carboxylated PEG-GATG copolymers, aggregation of CdSe NPs in serum, and citotoxicity of PEG-GATG copolymers. See DOI: 10.1039/b000000x/

1. M. Shen and X. Shi, *Nanoscale*, 2010, **2**, 1596-1610.
2. J. O. Winter, T. Y. Liu, B. A. Korgel and C. E. Schmidt, *Advanced Materials*, 2001, **13**, 1673-1677.
3. H. Bayley and P. S. Cremer, *Nature*, 2001, **413**, 226-230.
4. A. Haryono and W. H. Binder, *Small*, 2006, **2**, 600-611.
5. T. Selvan, J. P. Spatz, H.-A. Klok and M. Möller, *Advanced Materials*, 1998, **10**, 132-134.
6. J. P. Spatz, A. Roescher, S. Sheiko, G. Krausch and M. Möller, *Adv. Mater.*, 1995, **7**, 731-735.
7. J. J. Chiu, B. J. Kim, E. J. Kramer and D. J. Pine, *Journal of the American Chemical Society*, 2005, **127**, 5036-5037.
8. M. E. Garcia, L. A. Baker and R. M. Crooks, *Analytical Chemistry*, 1999, **71**, 256-258.
9. K. Esumi, A. Suzuki, N. Aihara, K. Usui and K. Torigoe, *Langmuir*, 1998, **14**, 3157-3159.

10. L. Balogh and D. A. Tomalia, *Journal of the American Chemical Society*, 1998, **120**, 7355-7356.
11. A. Fahmi, A. D'Aléo, R. M. Williams, L. De Cola, N. Gindy and F. Vögtle, *Langmuir*, 2007, **23**, 7831-7835.
12. A. Fahmi, T. Pietsch, D. Appelhans, N. Gindy and B. Voit, *New J. Chem.*, 2009, **33**, 703-706.
13. F. Wurm and H. Frey, *Progress in Polymer Science*, 2011, **36**, 1-52.
14. R. Vestberg, A. M. Piekarski, E. D. Pressly, K. Y. van Berkel, M. Malkoch, J. Gerbac, N. Ueno and C. J. Hawker, *J. Polym. Sci., Part A: Polym. Chem.*, 2009, **47**, 1237-1258.
15. A. Sousa-Herves, R. Riguera and E. Fernandez-Megia, *New Journal of Chemistry*, 2012, **36**, 205–210.
16. E. R. Gillies, T. B. Jonsson and J. M. J. Fréchet, *J. Am. Chem. Soc.*, 2004, **126**, 11936-11943.
17. Y. Yang, C. Hua and C.-M. Dong, *Biomacromolecules*, 2009, **10**, 2310-2318.
18. M. A. Carnahan, C. Middleton, J. Kim, T. Kim and M. W. Grinstaff, *J. Am. Chem. Soc.*, 2002, **124**, 5291-5293.
19. M. W. Grinstaff, *Biomaterials*, 2007, **28**, 5205-5214.
20. M. T. Morgan, M. A. Carnahan, S. Finkelstein, C. A. H. Prata, L. Degoricija, S. J. Lee and M. W. Grinstaff, *Chem. Commun.*, 2005, 4309-4311.
21. H. Namazi and S. Jafarirad, *Int. J. Pharm.*, 2011, **407**, 167-173.
22. A. Sousa-Herves, R. Novoa-Carballal, R. Riguera and E. Fernandez-Megia, *AAPS J.*, 2014, **16**, 948-961.
23. E. M. Munoz, J. Correa, E. Fernandez-Megia and R. Riguera, *J. Am. Chem. Soc.*, 2009, **131**, 17765-17767.
24. E. M. Munoz, J. Correa, R. Riguera and E. Fernandez-Megia, *J. Am. Chem. Soc.*, 2013, **135**, 5966-5969.
25. R. Novoa-Carballal, E. Säwén, E. Fernandez-Megia, J. Correa, R. Riguera and G. Widmalm, *Physical Chemistry Chemical Physics*, 2010, **12**, 6587-6589.
26. L. Albertazzi, M. Fernandez-Villamarin, R. Riguera and E. Fernandez-Megia, *Bioconjugate Chem.*, 2012, **23**, 1059-1068.
27. M. de la Fuente, M. Raviña, A. Sousa-Herves, J. Correa, R. Riguera, E. Fernandez-Megia, A. Sánchez and M. J. Alonso, *Nanomedicine*, 2012, **7**, 1667-1681.
28. M. Raviña, M. de la Fuente, J. Correa, A. Sousa-Herves, J. Pinto, E. Fernandez-Megia, R. Riguera, A. Sanchez and M. J. Alonso, *Macromolecules*, 2010, **43**, 6953-6961.
29. A. Sousa-Herves, E. Fernandez-Megia and R. Riguera, *Chem. Commun.*, 2008, 3136-3138.
30. F. Fernández-Trillo, J. Pacheco-Torres, J. Correa, P. Ballesteros, P. Lopez-Larrubia, S. Cerdán, R. Riguera and E. Fernandez-Megia, *Biomacromolecules*, 2011, **12**, 2902-2907.
31. R. Doménech, O. Abian, R. Bocanegra, J. Correa, A. Sousa-Herves, R. Riguera, M. G. Mateu, E. Fernandez-Megia, A. Velázquez-Campoy and J. L. Neira, *Biomacromolecules*, 2010, **11**, 2069-2078.
32. B. Klajnert, T. Wasiak, M. Ionov, M. Fernandez-Villamarin, A. Sousa-Herves, J. Correa, R. Riguera and E. Fernandez-Megia, *Nanomedicine (New York, NY, U. S.)*, 2012, **8**, 1372-1378.
33. V. V. Rostovtsev, L. G. Green, V. V. Fokin and K. B. Sharpless, *Angew. Chem., Int. Ed.*, 2002, **41**, 2596-2599.
34. C. W. Tornøe, C. Christensen and M. Meldal, *J. Org. Chem.*, 2002, **67**, 3057-3064.
35. E. Lallana, A. Sousa-Herves, F. Fernandez-Trillo, R. Riguera and E. Fernandez-Megia, *Pharm. Res.*, 2012, **29**, 1-34.
36. E. Lallana, F. Fernandez-Trillo, A. Sousa-Herves, R. Riguera and E. Fernandez-Megia, *Pharm. Res.*, 2012, **29**, 902-921.
37. E. Fernandez-Megia, J. Correa and R. Riguera, *Biomacromolecules*, 2006, **7**, 3104-3111.
38. M. De, P. S. Ghosh and V. M. Rotello, *Advanced Materials*, 2008, **20**, 4225-4241.
39. M. M. Alvarez, J. T. Khoury, T. G. Schaaff, M. N. Shafigullin, I. Vezmar and R. L. Whetten, *The Journal of Physical Chemistry B*, 1997, **101**, 3706-3712.
40. K. Esumi, A. Suzuki, A. Yamahira and K. Torigoe, *Langmuir*, 2000, **16**, 2604-2608.
41. T. Pietsch, D. Appelhans, N. Gindy, B. Voit and A. Fahmi, *Colloids and Surfaces A: Physicochemical and Engineering Aspects*, 2009, **341**, 93-102.
42. J. K. Lorenz, T. F. Kuech and A. B. Ellis, *Langmuir*, 1998, **14**, 1680-1683.
43. M. Tomasulo, I. Yildiz, S. L. Kaanumalle and F. M. Raymo, *Langmuir*, 2006, **22**, 10284-10290.
44. C. Bao, M. Jin, R. Lu, T. Zhang and Y. Y. Zhao, *Materials Chemistry and Physics*, 2003, **81**, 160-165.
45. D. A. Tomalia, *Prog. Polym. Sci.*, 2005, **30**, 294-324.
46. K. R. Gopidas, J. K. Whitesell and M. A. Fox, *J. Am. Chem. Soc.*, 2003, **125**, 14168-14180.
47. W. Guo, J. J. Li, Y. A. Wang and X. Peng, *J. Am. Chem. Soc.*, 2003, **125**, 3901-3909.
48. http://ncl.cancer.gov/NCL_Method_GTA-1.pdf.
49. V. Kumar, A. Kumari, P. Guleria and S. K. Yadav, in *Rev Environ Contam Toxicol*, 2012, vol. 215, pp. 39-121.
50. Á. França, B. Pelaz, M. Moros, C. Sánchez-Espinel, A. Hernández, C. Fernández-López, V. Grazú, J. M. de la Fuente, I. Pastoriza-Santos, L. M. Liz-Marzán and Á. González-Fernández, *Small*, 2010, **6**, 89-95.
51. A. M. Derfus, W. C. W. Chan and S. N. Bhatia, *Nano Letters*, 2003, **4**, 11-18.
52. F. M. Winnik and D. Maysinger, *Accounts of Chemical Research*, 2012, **46**, 672-680.
53. R. Weissleder, M. Nahrendorf and M. J. Pittet, *Nat Mater*, 2014, **13**, 125-138.
54. X. Duan and Y. Li, *Small*, 2013, **9**, 1521-1532.
55. A. Franca, P. Aggarwal, E. V. Barsov, S. V. Kozlov, M. A. Dobrovolskaia and A. Gonzalez-Fernandez, *Nanomedicine (London, U. K.)*, 2011, **6**, 1175-1188.
56. K. Knop, R. Hoogenboom, D. Fischer and U. S. Schubert, *Angew. Chem., Int. Ed.*, 2010, **49**, 6288-6308.
57. M. J. Joralemon, S. McRae and T. Emrick, *Chem. Commun.*, 2010, **46**, 1377-1393.
58. M. Moros, B. Hernaez, E. Garet, J. T. Dias, B. Saez, V. Grazu, A. Gonzalez-Fernandez, C. Alonso and J. M. de la Fuente, *ACS Nano*, 2012, **6**, 1565-1577.
59. B. Díaz, C. Sánchez-Espinel, M. Arruebo, J. Faro, E. de Miguel, S. Magadán, C. Yagüe, R. Fernández-Pacheco, M. R. Ibarra, J. Santamaría and Á. González-Fernández, *Small*, 2008, **4**, 2025-2034.